Bidirectional Catalysis by Copper-Containing Nitrite Reductase†

Hein J. Wijma,‡ Gerard W. Canters,‡ Simon de Vries,§ and Martin Ph. Verbeet*,‡

Leiden Institute of Chemistry, Leiden University, P.O. Box 9502, 2300 RA Leiden, The Netherlands, and Department of Biotechnology, Delft University of Technology, Julianalaan 67, 2628 BC Delft, The Netherlands

Received February 13, 2004; Revised Manuscript Received May 10, 2004

ABSTRACT: The copper-containing nitrite reductase from *Alcaligenes faecalis* S-6 was found to catalyze the oxidation of nitric oxide to nitrite, the reverse of its physiological reaction. Thermodynamic and kinetic constants with the physiological electron donor pseudoazurin were determined for both directions of the catalyzed reaction in the pH range of 6−8. For this, nitric oxide was monitored by a Clark-type electrode, and the redox state of pseudoazurin was measured by optical spectroscopy. The equilibrium constant (K_{eq}) depends on the reduction potentials of pseudoazurin and nitrite/nitric oxide, both of which vary with pH. Above pH 6.2 the formation of NiR substrates (nitrite and reduced pseudoazurin) is favored over the products (NO and oxidized pseudoazurin). At pH 8 the K_{eq} amounts to 10^3. The results show that dissimilatory nitrite reductases catalyze an unfavorable reaction at physiological pH (pH = 7−8). Consequently, nitrous oxide production by copper-containing nitrite reductases is unlikely to occur in vivo with a native electron donor. With increasing pH, the rate and specificity constant of the forward reaction decrease and become lower than the rate of the reverse reaction. The opposite occurs for the rate of the reverse reaction; thus the catalytic bias for nitrite reduction decreases. At pH 6.0 the k_{cat} for nitrite reduction was determined to be 1.5×10^3 s^{-1}, and at pH 8 the rate of the reverse reaction is 125 s^{-1}.

Denitrification is the part of the global nitrogen cycle in which fixed nitrogen is recycled to the atmosphere. It consists of the reduction of nitrate via nitrite, nitric oxide, and nitrous oxide to dinitrogen. Copper-containing nitrite reductases (NiR)[1] catalyze the reduction of nitrite to nitric oxide in a large variety of bacteria, archea, and fungi (*1*−*6*). Also in pathogens NiR is relevant; in *Neisseria gonorrhoeae* its expression enhances resistance against human sera (*7*). A second class, the cd_1 nitrite reductases, exists which have the same function in denitrification. The two types of nitrite reductase never occur in the same organism.

NiR catalyzes the one-electron reduction of nitrite to nitric oxide (eq 1a; pAZUox and pAZUred refer to oxidized and reduced pseudoazurin). We were interested in whether NiR would be capable of catalyzing the reverse reaction (eq 1b), a phenomenon to our knowledge not described before. Another question concerns the value of K_{eq} (eq 2) and how it depends on pH. Quantitative information on the thermodynamic constants relevant for NiR could help to understand the kinetic properties of the native enzyme and to interpret the effects of protein engineering.

$$\mathrm{NO} + \mathrm{pAZUox} + \mathrm{H_2O} \xrightarrow{\mathrm{NiR}} \mathrm{NO_2^-} + 2\mathrm{H^+} + \mathrm{pAZUred} \quad (1a)$$

$$\mathrm{NO_2^-} + 2\mathrm{H^+} + \mathrm{pAZUred} \xrightarrow{\mathrm{NiR}} \mathrm{NO} + \mathrm{pAZUox} + \mathrm{H_2O} \quad (1b)$$

$$K_{eq} = \frac{[\mathrm{NO}][\mathrm{pAZUox}]}{[\mathrm{NO_2^-}][\mathrm{pAZUred}]} \quad (2)$$

NiR is a trimer consisting of identical subunits (*8*). Each subunit contains a catalytic type 2 site (*9*) and a type 1 electron transfer site that accepts electrons and transfers these to the more buried type 2 site (*10*, *11*). For NiR from *Alcaligenes faecalis* S-6 (AfNiR) the physiological electron donor is pseudoazurin (pAZU) which contains a type 1 site and forms a complex with NiR via ionic and hydrophobic interactions (*12*−*15*). Kinetic and spectroscopic results suggest that the properties of the type 1 site change upon nitrite binding to the type 2 site and possibly the affinity of the type 2 site for nitrite increases upon binding of the physiological electron donor to NiR (*16*−*19*). In some enzymes the electron donor is fused to the NiR (*20*).

Three histidine nitrogens bind the type 2 copper in a tetrahedral geometry with the fourth position available for nitrite or water/hydroxyl to bind (*8*, *11*, *21*−*25*). Crystallographic and spectroscopic techniques show that the nitrite is bound to the copper via its oxygens while biomimetic models of the type 2 site always bind nitrite via the nitrogen atom (*5*, *16*, *17*, *22*, *23*, *26*). Residues His255, Asp98, and

† H.J.W. is supported by a Leiden Institute of Chemistry fellowship.

* Corresponding author. E-mail: verbeet@chem.leidenuniv.nl. Phone: (31) 71 527 4434. Fax: (31) 71 527 4349.

‡ Leiden University.

§ Delft University of Technology.

[1] Abbreviations: NiR, nitrite reductase; AfNiR nitrite reductase from *Alcaligenes faecalis* S-6; pAZUox, pseudoazurin from *A. faecalis* S-6 in its Cu^{2+} state; pAZUred, pseudoazurin from *A. faecalis* S-6 in its Cu^{1+} state; k_{cat}, catalytic constant; K_m, Michaelis constant; *R*, gas constant; *F*, Faraday constant.

10.1021/bi0496687 CCC: $27.50
Published on Web 07/20/2004

Ile/Val257 (AfNiR numbering) along with a water network in the active site are responsible for positioning the nitrite and reaction intermediates while donating protons (*21*, *25*, *27*, *28*).

An activity maximum at pH 6 is observed for Cu-containing nitrite reductases. Above pH 6 the catalytic rate decreases. It has been concluded that proton transfer is not rate limiting on the basis of the absence of a deuterium isotope effect (*17*). A number of other explanations have therefore been put forward to rationalize the decrease in rate above pH 6 (*29*−*32*): deprotonation of Asp98 and His255, or of the bound nitrite, or competitive inhibition by a hydroxyl ion.

To ascertain whether AfNiR could in fact catalyze the reverse reaction, the reaction was started with the normal products nitric oxide and oxidized pseudoazurin. Control experiments confirmed that the observed reaction was indeed the interconversion of NO_2^-/NO with reduced/oxidized pseudoazurin and that NiR catalyzed this reaction. This paper describes the kinetics and thermodynamics of the forward and reverse reaction catalyzed by NiR.

MATERIALS AND METHODS

Protein Expression and Purification. AfNiR was expressed and purified as described (*27*, *33*, *34*) with an extra gel filtration column (HiPrep S-200; Pharmacia Biosciences) added as the last step of the purification. For native AfNiR the final A_{280}/A_{460} ratio of 17 was identical to the previously reported value (*35*). The Cu content was 1.9 Cu atoms per monomer [determined with bicinchoninic acid (*36*)]. The expression and purification of the His145Ala AfNiR variant were described previously (*34*). In this NiR variant a ligand to the type 1 site was replaced, resulting in a type 1 copper site that is unable to transfer an electron to the catalytic type 2 site. Dr. Martin Boulanger and Prof. Dr Michael Murphy (Vancouver, Canada) cloned the gene for pseudoazurin from *A. faecalis* S-6 in a pET24a vector (*37*). The plasmid was expressed in *Escherichia coli* BL21(DE_3) grown in 2× YT medium at 30 °C. At an OD_{600} of 2 the temperature was lowered to 25 °C, and the culture was induced overnight by 0.5 mM IPTG. The purification protocol described by Kukimoto et al. (*12*) was followed. The final yield for different purifications was >200 mg/L of culture with an A_{277}/A_{593} ratio of 1.9−2.0, which is identical to the value reported for pure native protein (*12*, *14*).

Assays. Nitric oxide was monitored by a Clark-type electrode in a setup described by Girsch et al. (*38*). The source of nitric oxide was 5% NO in N_2 which at saturation gives 100 μM nitric oxide in H_2O at 25 °C. This 5% NO was passed through the anaerobic cell for 30 s. Prior to experiments the cell was left for a few minutes to determine the steady decrease of nitric oxide, which was caused by oxygen leaking into the cell.

Activities in the forward direction were measured at 25 °C using reduced pseudoazurin. Pseudoazurin was reduced with ascorbate, and excess reductant was removed by ultrafiltration with argon-flushed buffer. For pAZUred we determined the ϵ_{277} (=8200 mM^{-1} cm^{-1}) by titration with $K_3[Fe(CN)_6]$. The absorption at 593 nm [$\epsilon_{593} = 2900$ mM^{-1} cm^{-1} (*14*)] was used for calibration since this absorption peak does not overlap with the spectrum of $K_3[Fe(CN)_6]$. We observed that the absorption at 277 nm decreased upon titration with $K_3[Fe(CN)_6]$, consistent with the lower extinction coefficient for pAZUox [$\epsilon_{277} = 5700$ mM^{-1} cm^{-1} (*14*)]. For the determination of the K_m of nitrite, 315 μM pAZUred was used. For the K_m of pAZUred at least 2.5 mM nitrite was used. For assays in the reverse direction pAZUox was introduced in the buffer after oxygen was removed by repeated nitrogen/vacuum exposure. The buffer was 100 mM Mes/Hepes−NaOH. The pH of the solution was remeasured after the experiments. All reported activities were calculated from initial rates.

For all spectroscopic measurements in the presence of 100 μM NO, 1200 μL of buffer in a gastight cuvette was made anaerobic by flushing with nitrogen gas for 5 min, followed by flushing for 30 s with 5% nitric oxide in nitrogen. The top half of the cuvette was filled with 5% NO in N_2. Shaking the cuvette did not change the position of the equilibrium in Figures 2 and 3, suggesting that NO diffusion was sufficiently fast to keep the nitric oxide concentration in solution constant. A Hewlett-Packard HP-8452A spectrophotometer fitted with a diode array was used to record optical spectra. The reduction potential of pseudoazurin was determined by cyclovoltammetry with 4,4-dithiopyridine-modified gold as a working electrode (*39*, *40*).

Data Analysis. Equation 2 can be rearranged to give eq 3. For the fit of Figure 3B with eq 3 the concentration of nitric oxide was presumed to be 100 μM, and the presence of an initial concentration of nitrite was allowed for ($[NO_2^-]^{total} = [NO_2^-]^{initial} + [NO_2^-]^{added}$). The presence of nitrite prior to its addition was quantitatively confirmed with the Griess reagent (*41*) and is probably the result of oxygen leakage into the setup. The reduction potential of NO_2^-/NO_{aq} from Figure 4B could be calculated since it is coupled to the redox equilibrium of pseudoazurin (eqs 2 and 4 can be rearranged to eq 5).

$$[\text{pAZUox}] = \frac{[\text{pAZU}]_{\text{total}}}{\left(\frac{[\text{NO}]}{K_{\text{eq}}[\text{NO}_2^-]^{\text{total}}} + 1\right)} \tag{3}$$

$$E_{\text{NO}_2^-/\text{NO}} + \frac{RT}{F}\ln\left(\frac{[\text{NO}_2^-]}{[\text{NO}]}\right) = E_{\text{pAZU}} + \frac{RT}{F}\ln\left(\frac{[\text{pAZUox}]}{[\text{pAZUred}]}\right) \tag{4}$$

$$E_{\text{NO}_2^-/\text{NO}} = E_{\text{pAZU}} + \frac{RT}{F}\ln(K_{\text{eq}}) \tag{5}$$

For standard conditions (298 K, atmospheric pressure of gases, 1 M other reactants, including protons) the half-potential is $E_0 = 0.983$ V (*42*) for the reaction $HNO_2 + H^+ + e^- \rightarrow NO_g + H_2O$. With a $pK_a = 3.25$ the $E_0'_{pH7}$ of the NO_2^-/NO_g couple is then $0.983 - (3.25 \times 1 \times 2.3RT/F) - [(7 - 3.25) \times 2 \times 2.3RT/F] = 0.348$ V (*43*). This value is identical to the one calculated from the Gibbs free energy of formation from the elements (*44*). When the concentration of nitric oxide is expressed in moles per liter rather than partial pressure, the reduction potential is E_{m7} for $NO_2^-/NO_{aq} = 0.189$ V [obtained by substituting the concentration of nitric oxide in the water phase at 1 atm partial pressure, which amounts to 2.1 mM at 298 K: $E_{m7} = 0.348 + [\ln(0.0021)RT/F]$].

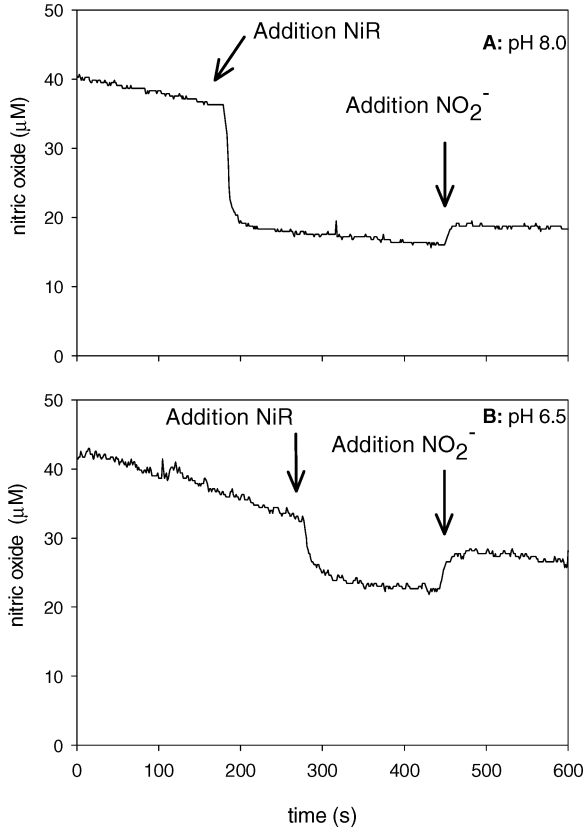

FIGURE 1: Nitric oxide consumption by pseudoazurin catalyzed by NiR. The *y*-axis displays the readings of the Clark electrode converted to nitric oxide concentration. The steady decrease is caused by oxygen leaking in. Pseudoazurin (20 μM) in its oxidized state was added prior to NiR (0.1 μM) and nitrite (2.5 mM). The Clark electrode adapts within 5−10 s to changes in nitric oxide concentration. Panels: A, pH 8.0; B, pH 6.5.

RESULTS

Figure 1A indicates that NiR does indeed catalyze the reverse reaction of nitric oxide to nitrite (eq 1b). Oxidized pseudoazurin and nitric oxide were mixed in solution while nitric oxide was monitored. Upon addition of NiR a sharp decrease in the concentration of NO was observed. Subsequent addition of nitrite made NO reappear, suggesting that the equilibrium shifted back toward the products (NO and pAZUox). Repeating the same experiment at lower pH (Figure 1B) yielded a smaller NO decrease; a relative larger amount of NO reappeared upon addition of nitrite. This pH effect was observed throughout pH 8−6.

Optical spectroscopy was used to observe the oxidized pseudoazurin (reduced pseudoazurin is colorless) while carrying out the same experiment as in Figure 1. Upon addition of NiR the concentration of pAZUox dropped to an equilibrium value (Figure 2). When nitrite was added, the equilibrium was shifted back toward oxidized pseudoazurin. The shape of the visible spectrum of the oxidized pseudoazurin remained identical during the experiment, indicating that no nitrite was bound to the pseudoazurin. The effect of pH on the position of the equilibrium was identical to that observed in Figure 1.

Control experiments were carried out to exclude that the observed activity for nitric oxide was caused by a contaminant such as a metal ion or some copurified activity. Addition of EDTA (8 mM) did not influence the rates or amplitudes

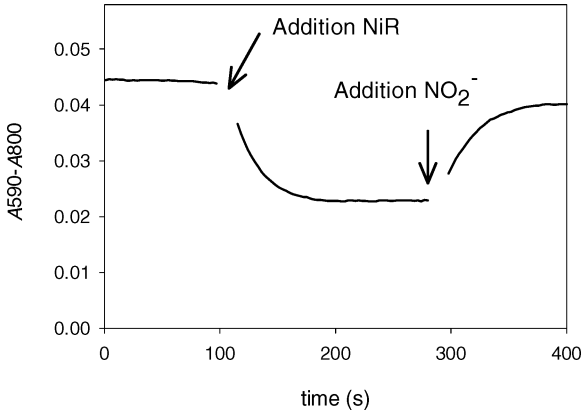

FIGURE 2: Equilibration of pAZUox/red in the presence of NiR. Nitric oxide and oxidized pseudoazurin are present prior to the addition of NiR (0.003 μM) and nitrite (8 mM). Reduction of pseudoazurin leads to loss of its absorbance in the visible region. The difference in absorbance between 590 (a peak position) and 800 nm was chosen to correct for baseline drifts.

observed with optical spectroscopy, indicating that no freely available metal ions catalyzed the reverse reaction. Furthermore, when the AfNiR mutant His145Ala (which has a very low catalytic activity due to an inactivated type 1 site) was used, no catalytic activity was observed, even in amounts a 100 times larger than that of native NiR. To exclude binding of nitric oxide to the type 1 site of pseudoazurin, a solution containing nitric oxide was titrated with pseudoazurin. The obtained absorption was linear with respect to added amounts of pseudoazurin and identical to the absorption in the absence of NO, showing that complex formation between the type 1 site and nitric oxide was absent.

To determine K_{eq} (eq 2), the concentration of pAZUox was monitored optically upon successive nitrite additions (Figure 3A). Increasing amounts of nitrite shifted the equilibrium toward pAZUox. The data could be fitted with eq 3 (Figure 3B). The values of K_{eq} hereby obtained decreased with increasing pH (Figure 3C). The slope of log(K_{eq}) versus pH was −1.6; this is close to the value of −2 expected when the consumption of two protons determines the equilibrium. The difference can be explained by taking into account the pH dependence of the reduction potential of pseudoazurin (vide infra). Above pH 6.2 the equilibrium constant is less than unity. At pH 8 the K_{eq} favored the formation of nitrite and pAZUred by a factor of 10^3 (Table 1).

To correlate the reduction potentials of pseudoazurin and nitrite/nitric oxide to K_{eq}, the reduction potential of pseudoazurin was measured. Between pH 6 and pH 8, the reduction potential of pseudoazurin decreased from 295 to 255 mV (Figure 4A). Filling in the determined values and K_{eq} into eq 5 resulted in the values for the reduction potential of nitrite/nitric oxide. A plot revealed a slope of -111 ± 5 mV per pH unit (Figure 4B). This is very close to the slope of 2×-59 mV per pH unit that is expected for a redox reaction in which two protons are consumed per electron (eq 6). The reduction potential for NO_2^-/NO_{aq} at pH 7 was found to be 202 ± 3 mV, which was in good agreement with the value calculated from standard conditions ($E_{m7} =$ 189 mV; see Materials and Methods).

$$NO_2^- + 2H^+ + e^- \rightarrow NO_{aq} + H_2O \qquad (6)$$

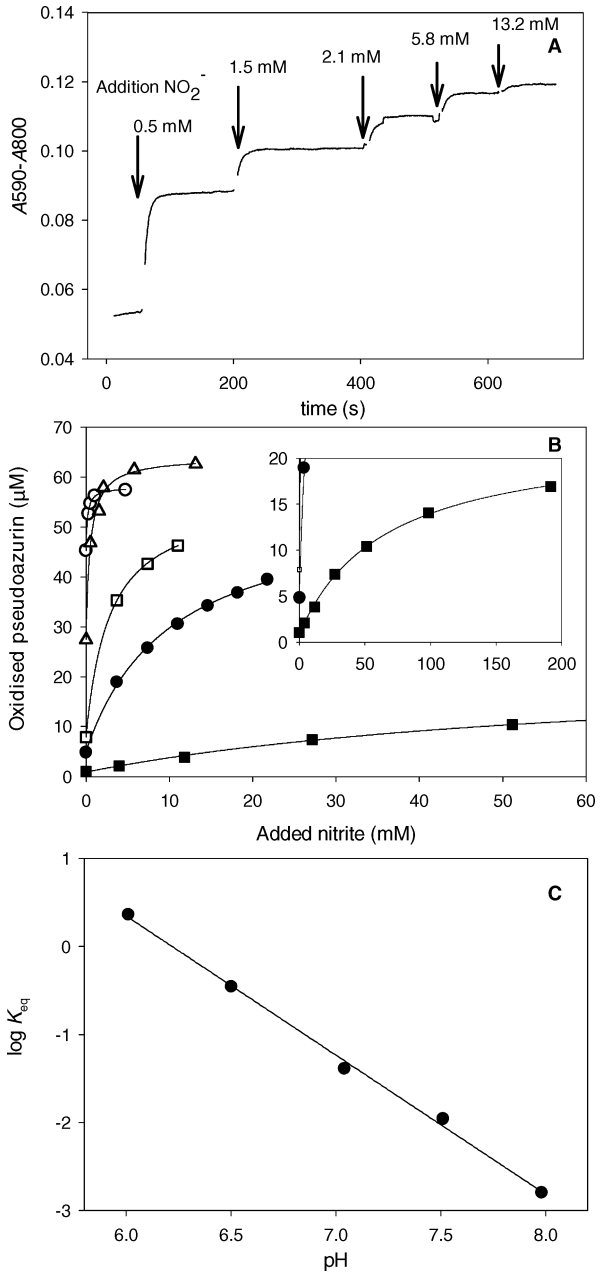

FIGURE 3: Determination of K_{eq} versus pH. Panel A: Titration of a mixture of pseudoazurin (65 μM) and nitric oxide (100 μM) with nitrite in the presence of a catalytic amount of nitrite reductase (0.1 μM). This was performed in Mes/Hepes buffer of 100 mM at pH 6.5. Panel B: Titration with nitrite at different pHs. Key: open circles, pH 6.0; open triangles, pH 6.5; open squares, pH 7.0; closed circles, pH 7.5; closed squares, pH 8.0. The total amount of pseudoazurin in the titration of pH 6−7.5 was 55−65 μM. For pH 8 this was 23 μM. The fit is according to eq 3. The inset shows the full range for pH 8.0. Panel C: Logarithmic plot of K_{eq} versus pH.

For a quantitative comparison with the thermodynamic constants obtained above, the catalytic constants for the rates of forward and reverse reaction and the Michaelis constants of nitrite, pAZUred, and pAZUox were determined. There was no indication for cooperative behavior of the NiR trimer throughout the pH range (Figure 5). For the forward reaction the catalytic constant (k_{cat}) drops dramatically with increasing pH (Table 1). The K_m for nitrite had a minimum at pH 7 at 35 μM but increased to 220 μM at pH 8. For pAZUred the K_m varied with pH between 70 and 155 μM. The specificity constant (k_{cat}/K_m) for nitrite and pAZUred decreased from 10^7 M^{-1} s^{-1} at pH 6 to 10^5 M^{-1} s^{-1} at pH 8.

The rate of the reverse reaction increased with pH. The catalytic bias for nitrite reduction [k_{cat}(forward)/k_{cat}(reverse)] decreased toward more alkaline pH (Table 1). At pH 8 the catalytic bias of NiR was toward nitric oxide oxidation. The rate constant for nitric oxide oxidation at pH 8.0 was 10 times lower (125 s^{-1}) than the rate constant for the forward reaction at pH 6.0. At pH 6.0 we could not determine a reliable rate for the reverse reaction. At lower concentrations of pAZUox (<20 μM) no reliable initial rates could be obtained. The K_m for pAZUox is calculated to be below 15 μM at pH 7.5 and 8.0 since above 25 μM pAZUox no change in activity was observed.

DISCUSSION

Bidirectional Catalysis. Here it is found for the first time that NiR can catalyze bidirectionally. Considering the high reactivity of nitric oxide with transition metals, it was necessary to exclude that a contaminant or a copurified activity was responsible for the observed activity in the reverse direction. Likely culprits, such as $Cu^{1+/2+}$, would be complexed by EDTA; addition of the latter did not change activity, making such a contaminant unlikely. A titration of pseudoazurin with NO excluded that nitric oxide forms a Cu^{2+}−NO complex with the type 1 site of pseudoazurin at room temperature as it does with azurin at 77 K (*45*). The AfNiR variant His145Ala was useful as a negative control since it has a 100000-fold lower catalytic activity than native NiR (0.0022 s^{-1} at pH 6.5; unpublished results) while only the structure of the type 1 site is influenced by the mutation (*34*). For NiR H145A no reverse activity was observed, confirming that the native NiR catalyzed the oxidation of NO to NO_2^-.

The stoichiometry of the reaction could be determined since nitric oxide and pseudoazurin were observed directly while the involvement of nitrite and two protons could be inferred from their effect on the position on K_{eq} (Figure 3). The reduction potential of 202 mV found in Figure 4B was in agreement with the E_{m7} = 189 mV for the reaction $2H^+ + NO_2^- + e^- \rightarrow NO_{aq}$ (not to be confused with the standard reduction potential $E_0'_{pH7.0}$ = 348 mV, which equals the potential of a solution containing 1 M nitrite and 2.1 mM nitric oxide; see Materials and Methods). The consumption of two protons per electron in the reaction of NO_2^-/NO is expected to cause a −118 mV ($-2 \times 2.3RT/F$) per pH unit dependence of its reduction potential, very close to the observed value of −111 mV per pH unit. The value of K_{eq} is determined by the difference in reduction potential between nitrite and pseudoazurin (eq 5). Since pseudoazurin has a higher reduction potential than nitrite above pH 6.2, the equilibrium favored the formation of the substrates (pAZUred and NO_2^-) above this pH. The stoichiometry determined here for the catalyzed equilibrium corresponds to that in eq 1 and is well established for Cu-containing and cd_1 nitrite reductases (*1*).

The Electron Donor. The reduction potential at pH 7 of pseudoazurin was determined to be 270 mV, which is identical to that measured previously for *A. faecalis* pseudoazurin (*12*). We observed that the reduction potential of pseudoazurin decreased slightly with pH. The dependence on pH is very similar to that observed for the pseudoazurin

Table 1: Kinetic and Equilibrium Constants for AfNiR versus pH[a]

pH	k_{cat}(forward) (s^{-1})	K_m(pAZUred) (μM)	$K_m(NO_2^-)$ (μM)	$k_{cat}/K_m(NO_2^-)$ (10^6 M^{-1} s^{-1})	k_{cat}/K_m(pAZUred) (10^6 M^{-1} s^{-1})	k_{cat}(reverse) (s^{-1})	K_m(pAZUox) (μM)	K_{eq}	catalytic bias
6.0	1478 ± 54	67 ± 8	49 ± 5	30.1	22.1	ND	ND	2.3	ND
6.5	1046 ± 33	77 ± 8	53 ± 5	19.7	13.5	38	ND	0.35	28
7.0	392 ± 6	102 ± 10	36 ± 2	10.9	3.85	64	ND	0.041	6.1
7.5	219 ± 6	156 ± 19	68 ± 7	3.21	1.41	109	<15	0.011	2.0
8.0	71 ± 2	85 ± 12	221 ± 24	0.32	0.84	125	<15	0.0016	0.57

[a] All measurements were done in 100 mM Mes/Hepes buffers. ND, not determined. Catalytic bias = k_{cat}(forward)/k_{cat}(reverse).

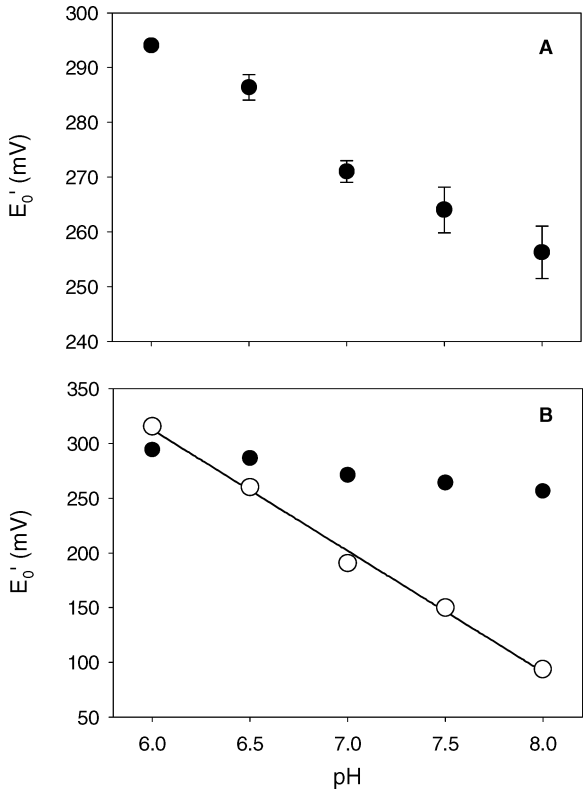

FIGURE 4: Reduction potential of pseudoazurin and nitrite versus pH. The reduction potential of pseudoazurin was determined by cyclovoltammetry in the same buffer (Mes/Hepes, 100 mM) as was used for the activity and the equilibration assays. The reduction potential of nitrite was calculated with the Nernst equation from the reduction potential of pseudoazurin and K_{eq}. Panel A: Reduction potential of pseudoazurin (closed circles with error bars). Panel B: Reduction potential of nitrite (open circles; fitted with a least-squares fit to the data points; see text for further details). The reduction potential of pseudoazurin (closed circles) is plotted for reference.

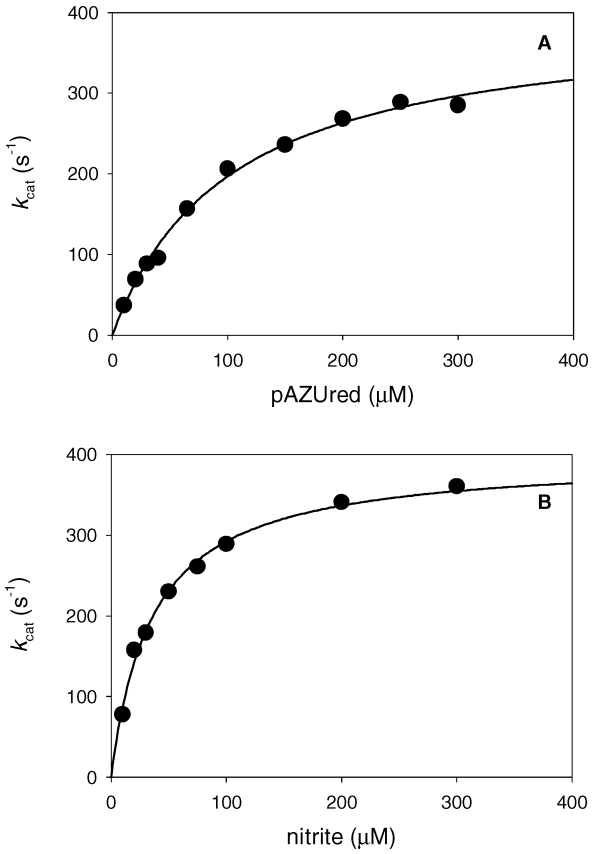

FIGURE 5: Determination of k_{cat} and K_m for nitrite and reduced pseudoazurin. Panel A: Activity versus nitrite concentration at pH 7. Panel B: Activity versus pAZUred at pH 7. See Materials and Methods for experimental details.

Table 2: Reduction Potentials for Electron Donors to Nitrite Reductases[a]

E_0' (mV)	classification	origin	redox partner
305	azurin	*A. xylosoxidans*	Cu NiR
265	cyt *c*-551	*Pseudomonas aeruginosa*	cd_1 NiR
265	cyt *c*-552	*Pseudomonas nautica*	cd_1 NiR
270	pseudoazurin	*A. cycloclastes*	Cu NiR
230	pseudoazurin	*Paracoccus pantotrophus*	cd_1 NiR
270	pseudoazurin	*A. faecalis* S-6	Cu NiR

[a] Reduction potentials (at or near pH 7) were taken from refs *12*, *40*, and *60*−*63*. Cu NiR, copper-containing nitrite reductase; cd_1, *c* and d_1 heme-containing nitrite reductase.

from *Achromobacter cycloclastes* (*40*). For this pseudoazurin, Sato and Dennison (*40*) showed the reduction potential to depend on the protonation of His6. The same explanation is likely to hold here since this histidine is conserved in *A. faecalis* pAZU and the proteins are closely related (65% identical amino acid sequence).

The electron donors for other nitrite reductases have also reduction potentials higher than the reduction potential for NO_2^-/NO_{aq} (Table 2). Table 2 shows that the electron donors for Cu-containing and cd_1 nitrite reductases have very similar reduction potentials. This implies that it is common for nitrite reductases to catalyze an unfavorable reaction. This is especially true in the physiologically important pH range 7−8, which is optimal for denitrification (*46*).

Catalysis by Nitrite Reductase. The value of k_{cat} (1.5 × 10^3 s^{-1}) measured at pH 6.0 is similar to the activity measured for *Alcaligenes xylosoxidans* (1.6 × 10^3 s^{-1}) (*29*). Furthermore, at pH 7.0 the measured 392 s^{-1} equals the 387 s^{-1} reported for AfNiR at this pH (*13*). The catalytic rate at pH 6.0 (1500 s^{-1}) is also in agreement with the rates measured for electron transfer between the type 1 and type 2 site of nitrite reductase from other sources, which is up to

2100 s^{-1} (*2*). Also the dependence of k_{cat} on pH found here with the physiological electron donor is similar to that reported with the artificial electron donor methyl viologen (*35*). For AfNiR a K_m for nitrite of 74 μM (pH 7.0, methyl viologen as electron donor) is reported, which differs significantly from the value we obtained at pH 7.0 with pseudoazurin as the electron donor (35.8 ± 2.1 μM). This is not unexpected since also for cd_1 nitrite reductase it is observed that the electron donor influences the K_m for nitrite (*47*). The data obtained here thus agree with those reported for this and other Cu-containing nitrite reductases.

One of the explanations for the decreased activity above pH 6 is competitive inhibition by the hydroxyl ion. The binding of hydroxyl is observed in a crystal structure at pH 8.5 (*31*). Hydroxyl ion inhibition is also suggested to explain a decrease in activity at high pH in the Cu-containing active site of laccase (*48*). Competitive inhibition by hydroxyl ion is expected to increase the K_m for nitrite by a factor 10 per pH unit while the k_{cat} is not affected (*49*). Here we find that after a minimum is reached at pH 7, the K_m for nitrite has increased an order of magnitude at pH 8 (Table 1). This observation supports a significant role for hydroxyl inhibition above pH 7.

In assays employing the artificial electron donor phenazine metasulfate (PMS) (*35*, *50*) nitrous oxide is found as a product in addition to nitric oxide. Careful analysis showed that NiR catalyzes the reaction $NO + NO_2^- + 4H^+ + 3e^- \rightarrow N_2O + 2H_2O$ when nitric oxide builds up in concentration (*50*). With PMS ($E_0' = 92$ mV) as an electron donor the equilibrium is much further to the formation of nitric oxide than with a physiological electron donor ($E_0' = 230-305$ mV). In *A. cycloclastes* the concentration of nitric oxide is indeed very low during denitrification: 9−30 nM when grown on nitrite (*51*). Thus, the production of nitrous oxide is unlikely to occur via NiR with its natural electron donors; their high reduction potentials (Table 2) make it impossible to reach high concentrations of NO.

Catalytic Bias. Since an enzyme cannot alter the equilibrium constant of its substrate and products, an enzyme must catalyze both the forward and reverse reaction at rates that conform to the equilibrium. As a result, the k_{cat} and the affinity constants for the forward and the reverse reaction are related to K_{eq} via one or more Haldane relationship(s) (*49*, *52*). For any catalyzed reaction, there is always a Haldane relationship in which the catalytic constant for the forward reaction is in the numerator and the catalytic constant for the reverse reaction is in the denominator combined with one or more (depending on the catalytic mechanism) Michaelis and inhibition constants (*52*). For example, for the most simple enzyme-catalyzed reaction with a single substrate and product in variable concentration, the appropriate Haldane relationship is $K_{eq} = (k_{cat}/K_m)^{forward}/(k_{cat}/K_m)^{reverse}$. Therefore, enzymes can have an intrinsic catalytic bias (higher k_{cat} in a particular direction of the reaction). AfNiR has an intrinsic catalytic bias near pH 6.2 where K_{eq} approaches unity ($k_{cat}^{nitrite}/k_{cat}^{nitric\ oxide} > 25$, at pH 6.5; Table 1).

Haldane relationships clarify why a redox enzyme can tune its intrinsic catalytic bias partly by the difference between the reduction potential of the substrate and the active site. The difference between these reduction potentials determines the equilibrium concentrations of the oxidized/reduced active site over the oxidized/reduced substrate and, thus, determines the equilibrium rates of substrate reduction over active site reduction. The catalytic bias of an enzyme would be determined entirely by the difference between the reduction potentials of the active site and the substrate if all affinity constants for the substrate were identical to that of the product and if the catalytic rates in the active site were fully rate-determining for the enzyme. Although these conditions are never completely fulfilled in enzymes, in general the difference between the reduction potentials of the active site and the substrate correctly predicts the intrinsic catalytic bias of an enzyme, and the catalytic bias can be modeled accurately when the dissociation constants for substrate and product are known (*53*−*58*).

For AfNiR we observe that the catalytic bias for nitrite reduction decreases at increasing pH, and at pH 8 AfNiR is biased toward nitric oxide oxidation (Table 1). A similar pH-dependent switch of the catalytic bias from substrate reduction to product oxidation was also observed for succinate dehydrogenase and [Ni-Fe] hydrogenase, where it was shown to be dependent on the difference in reduction potential between the active site and substrate (*57*, *58*). For NiRs from different sources reduction potentials of the catalytic type 2 sites have been determined to vary from <200 mV (upper limit determined by redox titration) to 250−280 mV (values determined by pulse radiolysis) (*2*, *59*) at pH 7.0. The reduction potential of the type 2 site of NiR decreases 60 mV between pH 6 and pH 7 and becomes constant above pH 7 (*32*). At pH 6.0, the substrate couple NO_2^-/NO_{aq} with 307 mV has a higher reduction potential than the type 2 site. The decreasing bias for nitrite reduction at increasing pH is consistent with the 118 mV per pH unit decrease in reduction potential of nitrite/nitric oxide, while the reduction potential of the type 2 site decreases far less. Although other factors could be involved as well, also in NiR the catalytic bias appears to be predicted by the difference in reduction potential between the active site and substrate.

Conclusions. The results reported here show that copper-containing NiR can catalyze its reverse reaction very well. The value of K_{eq} of nitrite/nitric oxide and reduced and oxidized pseudoazurin favored the formation of reduced pseudoazurin and nitrite above pH 6.2. Toward more alkaline pH, the catalytic bias for nitrite reduction decreased, and at pH 8 nitric oxide oxidation was faster than nitrite reduction. Comparison with the known reduction potentials of electron donors indicated that all dissimilatory nitrite reductases catalyze an unfavorable reaction. Nitrous oxide formation by NiR (*50*) is unlikely to occur with a natural electron donor since nitric oxide will not reach high enough concentrations. Above pH 7 competitive inhibition by hydroxyl appeared to be important for the K_m for nitrite. The results may help to design and interpret protein engineering experiments.

ACKNOWLEDGMENT

We acknowledge Marc Stampraad for assistance with the Clark-type electrode and Jonathan A. R. Worrall for commenting on the manuscript.

REFERENCES

1. Zumft, W. G. (1997) Cell biology and molecular basis of denitrification, *Microbiol. Mol. Biol. Rev. 61*, 533−616.

2. Suzuki, S., Kataoke, K., Yamaguchi, K., Inoue, T., and Kai, Y. (1999) Structure−function relationships of copper-containing nitrite reductases, *Coord. Chem. Rev. 190*−*192*, 245−265.
3. Adman, E. T. (1991) Copper protein structures, *Adv. Protein Chem. 42*, 145−197.
4. Ichiki, H., Tanaka, Y., Mochizuki, K., Yoshimatsu, K., Sakurai, T., and Fujiwara, T. (2001) Purification, characterization, and genetic analysis of Cu-containing dissimilatory nitrite reductase from a denitrifying halophilic archaeon, *Haloarcula marismortui*, *J. Bacteriol. 183*, 4149−4156.
5. Wasser, I. M., de Vries, S., Moenne-Loccoz, P., Schroder, I., and Karlin, K. D. (2002) Nitric Oxide in Biological Denitrification: Fe/Cu Metalloenzyme and Metal Complex NOx Redox Chemistry, *Chem. Rev. 102*, 1201−1234.
6. Averill, B. A. (1996) Dissimilatory Nitrite and Nitric Oxide Reductases, *Chem. Rev. 96*, 2951−2964.
7. Cardinale, J. A., and Clark, V. L. (2000) Expression of AniA, the major anaerobically induced outer membrane protein of *Neisseria gonorrhoeae*, provides protection against killing by normal human sera, *Infect. Immun. 68*, 4368−4369.
8. Godden, J. W., Turley, S., Teller, D. C., Adman, E. T., Liu, M. Y., Payne, W. J., and LeGall, J. (1991) The 2.3 angstrom X-ray structure of nitrite reductase from *Achromobacter cycloclastes*, *Science 253*, 438−442.
9. Libby, E., and Averill, B. A. (1992) Evidence that the type 2 copper centers are the site of nitrite reduction by *Achromobacter cycloclastes* nitrite reductase, *Biochem. Biophys. Res. Commun. 187*, 1529−1535.
10. Murphy, M. E., Turley, S., Kukimoto, M., Nishiyama, M., Horinouchi, S., Sasaki, H., Tanokura, M., and Adman, E. T. (1995) Structure of *Alcaligenes faecalis* nitrite reductase and a copper site mutant, M150E, that contains zinc, *Biochemistry 34*, 12107−12117.
11. Kukimoto, M., Nishiyama, M., Murphy, M. E., Turley, S., Adman, E. T., Horinouchi, S., and Beppu, T. (1994) X-ray structure and site-directed mutagenesis of a nitrite reductase from *Alcaligenes faecalis* S-6: roles of two copper atoms in nitrite reduction, *Biochemistry 33*, 5246−5252.
12. Kukimoto, M., Nishiyama, M., Ohnuki, T., Turley, S., Adman, E. T., Horinouchi, S., and Beppu, T. (1995) Identification of interaction site of pseudoazurin with its redox partner, copper-containing nitrite reductase from *Alcaligenes faecalis* S-6, *Protein Eng. 8*, 153−158.
13. Kukimoto, M., Nishiyama, M., Tanokura, M., Adman, E. T., and Horinouchi, S. (1996) Studies on protein−protein interaction between copper-containing nitrite reductase and pseudoazurin from *Alcaligenes faecalis* S-6, *J. Biol. Chem. 271*, 13680−13683.
14. Kakutani, T., Watanabe, H., Arima, K., and Beppu, T. (1981) A blue protein as an inactivating factor for nitrite reductase from *Alcaligenes faecalis* strain S-6, *J. Biochem. (Tokyo) 89*, 463−472.
15. Impagliazzo, A., and Ubbink, M. (2004) Mapping of the binding site on pseudoazurin in the transient 152 kDa complex with nitrite reductase, *J. Am. Chem. Soc. 126*, 5658−5659.
16. Veselov, A., Olesen, K., Sienkiewicz, A., Shapleigh, J. P., and Scholes, C. P. (1998) Electronic structural information from Q-band ENDOR on the type 1 and type 2 copper liganding environment in wild-type and mutant forms of copper-containing nitrite reductase, *Biochemistry 37*, 6095−6105.
17. Zhao, Y., Lukoyanov, D. A., Toropov, Y. V., Wu, K., Shapleigh, J. P., and Scholes, C. P. (2002) Catalytic function and local proton structure at the type 2 copper of nitrite reductase: the correlation of enzymatic pH dependence, conserved residues, and proton hyperfine structure, *Biochemistry 41*, 7464−7474.
18. Strange, R. W., Murphy, L. M., Dodd, F. E., Abraham, Z. H., Eady, R. R., Smith, B. E., and Hasnain, S. S. (1999) Structural and kinetic evidence for an ordered mechanism of copper nitrite reductase, *J. Mol. Biol. 287*, 1001−1009.
19. Prudêncio, M., Eady, R. R., and Sawers, G. (2001) Catalytic and spectroscopic analysis of blue copper-containing nitrite reductase mutants altered in the environment of the type 2 copper centre: implications for substrate interaction, *Biochem. J. 353*, 259−266.
20. Yamaguchi, K., Kobayashi, M., Kataoka, K., and Suzuki, S. (2003) Characterization of two Cu-containing protein fragments obtained by limited proteolysis of *Hyphomicrobium denitrificans* A3151 nitrite reductase, *Biochem. Biophys. Res. Commun. 300*, 36−40.
21. Boulanger, M. J., Kukimoto, M., Nishiyama, M., Horinouchi, S., and Murphy, M. E. (2000) Catalytic roles for two water bridged residues (Asp-98 and His-255) in the active site of copper-containing nitrite reductase *J. Biol. Chem. 275*, 23957−23964.
22. Murphy, M. E., Turley, S., and Adman, E. T. (1997) Structure of nitrite bound to copper-containing nitrite reductase from *Alcaligenes faecalis*. Mechanistic implications, *J. Biol. Chem. 272*, 28455−28460.
23. Adman, E. T., Godden, J. W., and Turley, S. (1995) The structure of copper-nitrite reductase from *Achromobacter cycloclastes* at five pH values, with NO_2^- bound and with type II copper depleted, *J. Biol. Chem. 270*, 27458−27474.
24. Inoue, T., Gotowda, M., Deligeer, Kataoka, K., Yamaguchi, K., Suzuki, S., Watanabe, H., Gohow, M., and Kai, Y. (1998) Type 1 Cu structure of blue nitrite reductase from *Alcaligenes xylosoxidans* GIFU 1051 at 2.05 Å resolution: Comparison of blue and green nitrite reductases, *J. Biochem. (Tokyo) 124*, 876−879.
25. Dodd, F. E., Van Beeumen, J., Eady, R. R., and Hasnain, S. S. (1998) X-ray structure of a blue-copper nitrite reductase in two crystal forms. The nature of the copper sites, mode of substrate binding and recognition by redox partner, *J. Mol. Biol. 282*, 369−382.
26. Howes, B. D., Abraham, Z. H., Lowe, D. J., Bruser, T., Eady, R. R., and Smith, B. E. (1994) EPR and electron nuclear double resonance (ENDOR) studies show nitrite binding to the type 2 copper centers of the dissimilatory nitrite reductase of *Alcaligenes xylosoxidans* (NCIMB 11015), *Biochemistry 33*, 3171−3177.
27. Boulanger, M. J., and Murphy, M. E. (2001) Alternate substrate binding modes to two mutant (D98N and H255N) forms of nitrite reductase from *Alcaligenes faecalis* S-6: Structural model of a transient catalytic intermediate, *Biochemistry 40*, 9132−9141.
28. Boulanger, M. J., and Murphy, M. E. P. (2003) Directing the mode of nitrite binding to a copper-containing nitrite reductase from *Alcaligenes faecalis* S-6: Characterization of an active site isoleucine, *Protein Sci. 12*, 248−256.
29. Kataoka, K., Furusawa, H., Takagi, K., Yamaguchi, K., and Suzuki, S. (2000) Functional analysis of conserved aspartate and histidine residues located around the type 2 copper site of copper-containing nitrite reductase, *J. Biochem. (Tokyo) 127*, 345−350.
30. Zhang, H. M., Boulanger, M. J., Mauk, A. G., and Murphy, M. E. P. (2000) Carbons monoxide binding to copper-containing nitrite reductase from *Alcaligenes faecalis*, *J. Phys. Chem. B 104*, 10738−10742.
31. Ellis, M. J., Dodd, F. E., Strange, R. W., Prudencio, M., Sawers, G., Eady, R. R., and Hasnain, S. S. (2001) X-ray structure of a blue copper nitrite reductase at high pH and in copper-free form at 1.9 Å resolution, *Acta Crystallogr., Sect. D: Biol. Crystallogr. 57*, 1110−1118.
32. Kobayashi, K., Tagawa, S., Deligeer, and Suzuki, S. (1999) The pH-dependent changes of intramolecular electron transfer on copper-containing nitrite reductase, *J. Biochem. (Tokyo) 126*, 408−412.
33. Nishiyama, M., Suzuki, J., Kukimoto, M., Ohnuki, T., Horinouchi, S., and Beppu, T. (1993) Cloning and characterization of a nitrite reductase gene from *Alcaligenes faecalis* and its expression in *Escherichia coli*, *J. Gen. Microbiol. 139*, 725−733.
34. Wijma, H. J., Boulanger, M. J., Molon, A., Fittipaldi, M., Huber, M., Murphy, M. E., Verbeet, M. P., and Canters, G. W. (2003) Reconstitution of the type-1 active site of the H145G/A variants of nitrite reductase by ligand insertion, *Biochemistry 42*, 4075−4083.
35. Kakutani, T., Watanabe, H., Arima, K., and Beppu, T. (1981) Purification and properties of a copper-containing nitrite reductase from a denitrifying bacterium, *Alcaligenes faecalis* strain S-6, *J. Biochem. (Tokyo) 89*, 453−461.
36. Brenner, A. J., and Harris, E. D. (1995) A quantitative test for copper using bicinchoninic acid, *Anal. Biochem. 226*, 80−84 [erratum (1995) *Anal. Biochem. 230*, 360].
37. Prudêncio, M., Rohovec, J., Peters, J. A., Tocheva, E., Boulanger, M. J., Murphy, M. E. P., Hupkes, H., Kosters, W., Impagliazzo, A., and Ubbink, M. (2004) A caged lanthanide complex as a paramagnetic shift agent for protein NMR, *Chem. Eur. J. 10*, 3252−3260.
38. Girsch, P., and de Vries, S. (1997) Purification and initial kinetic and spectroscopic characterization of NO reductase from *Paracoccus denitrificans*, *Biochim. Biophys. Acta 1318*, 202−216.
39. Dennison, C., Kohzuma, T., McFarlane, W., Suzuki, S., and Sykes, A. G. (1994) Reactivity of pseudoazurin from *Achromobacter cycloclastes* with inorganic redox partners and related NMR and electrochemical studies, *Inorg. Chem. 33*, 3299−3305.

40. Sato, K., and Dennison, C. (2002) Effect of histidine 6 protonation on the active site structure and electron-transfer capabilities of pseudoazurin from *Achromobacter cycloclastes*, *Biochemistry 41*, 120−130.
41. Nicholas, D. J. D., and Nason, A. (1957) Determination of nitrate and nitrite, *Methods Enzymol. 3*, 981−984.
42. Lide, D. R. (2001) *CRC Handbook of Chemistry and Physics*, 82nd ed., CRC Press, Boca Raton, London, New York, and Washington, DC.
43. Clark, W. M. (1960) *Oxidation−Reduction Potentials of Organic Systems*, Williams & Wilkins, Baltimore, MD.
44. Thauer, R. K., Jungermann, K., and Decker, K. (1977) Energy Conservation in chemotrophic anaerobic bacteria, *Bacteriol. Rev. 41*, 100−180.
45. Gorren, A. C., de Boer, E., and Wever, R. (1987) The reaction of nitric oxide with copper proteins and the photodissociation of copper-NO complexes, *Biochim. Biophys. Acta 916*, 38−47.
46. Knowles, R. (1982) Denitrification, *Microbiol. Rev. 46*, 43−70.
47. Richter, C. D., Allen, J. W., Higham, C. W., Koppenhofer, A., Zajicek, R. S., Watmough, N. J., and Ferguson, S. J. (2002) Cytochrome cd1, reductive activation and kinetic analysis of a multifunctional respiratory enzyme, *J. Biol. Chem. 277*, 3093−3100.
48. Xu, F. (1997) Effects of redox potential and hydroxide inhibition on the pH activity profile of fungal laccases, *J. Biol. Chem. 272*, 924−928.
49. Fersht, A. (1999) *Structure and Mechanism in Protein Science*, 1st ed., W. H. Freeman, New York.
50. Jackson, M. A., Tiedje, J. M., and Averill, B. A. (1991) Evidence for a NO-rebound mechanism for production of N2O from nitrite by the copper-containing nitrite reductase from *Achromobacter cycloclastes*, *FEBS Lett. 291*, 41−44.
51. Goretski, J., Zafiriou, O. C., and Hollocher, T. C. (1990) Steady-state nitric oxide concentrations during denitrification, *J. Biol. Chem. 265*, 11535−11538.
52. Cleland, W. W. (1963) The kinetics of enzyme-catalyzed reactions with two or more substrates or products, *Biochim. Biophys. Acta 67*, 104−137.
53. Heering, H. A., Hirst, J., and Armstrong, F. A. (1998) Interpreting the catalytic voltammetry of electroactive enzymes adsorbed on electrodes, *J. Phys. Chem. B 102*, 6889−6902.
54. Hagedoorn, P. L., Hagen, W. R., Stewart, L. J., Docrat, A., Bailey, S., and Garner, C. D. (2003) Redox characteristics of the tungsten DMSO reductase of *Rhodobacter capsulatus*, *FEBS Lett. 555*, 606−610.
55. Leger, C., Heffron, K., Pershad, H. R., Maklashina, E., Luna-Chavez, C., Cecchini, G., Ackrell, B. A., and Armstrong, F. A. (2001) Enzyme electrokinetics: energetics of succinate oxidation by fumarate reductase and succinate dehydrogenase, *Biochemistry 40*, 11234−11245.
56. Sucheta, A., Ackrell, B. A., Cochran, B., and Armstrong, F. A. (1992) Diode-like behaviour of a mitochondrial electron-transport enzyme, *Nature 356*, 361−362.
57. Hirst, J., Ackrell, B. A. C., and Armstrong, F. A. (1997) Global observation of hydrogen/deuterium isotope effects on bidirectional catalytic electron transport in an enzyme: Direct measurement by protein-film voltammetry, *J. Am. Chem. Soc. 119*, 7434−7439.
58. Hirst, J., Sucheta, A., Ackrell, B. A. C., and Armstrong, F. A. (1996) Electrocatalytic voltammetry of succinate dehydrogenase: Direct quantification of the catalytic properties of a complex electron-transport enzyme, *J. Am. Chem. Soc. 118*, 5031−5038.
59. Olesen, K., Veselov, A., Zhao, Y., Wang, Y., Danner, B., Scholes, C. P., and Shapleigh, J. P. (1998) Spectroscopic, kinetic, and electrochemical characterization of heterologously expressed wild-type and mutant forms of copper-containing nitrite reductase from *Rhodobacter sphaeroides* 2.4.3, *Biochemistry 37*, 6086−6094.
60. Dodd, F. E., Hasnain, S. S., Hunter, W. N., Abraham, Z. H., Debenham, M., Kanzler, H., Eldridge, M., Eady, R. R., Ambler, R. P., and Smith, B. E. (1995) Evidence for two distinct azurins in *Alcaligenes xylosoxidans* (NCIMB 11015): potential electron donors to nitrite reductase, *Biochemistry 34*, 10180−10186.
61. Horio, T., Higashi, T., Sasagawa, M., Kusai, K., Nakai, M., and Okunuki, K. (1960) Preparation of crystalline *Pseudomonas* cytochrome *c*-551 and its general properties, *Biochem. J. 77*, 194−201.
62. Lopes, H., Besson, S., Moura, I., and Moura, J. J. (2001) Kinetics of inter- and intramolecular electron transfer of *Pseudomonas nautica* cytochrome cd1 nitrite reductase: regulation of the NO-bound end product, *J. Biol. Inorg. Chem. 6*, 55−62.
63. Moir, J. W., Baratta, D., Richardson, D. J., and Ferguson, S. J. (1993) The purification of a cd_1-type nitrite reductase from, and the absence of a copper-type nitrite reductase from, the aerobic denitrifier *Thiosphaera pantotropha*; the role of pseudoazurin as an electron donor, *Eur. J. Biochem. 212*, 377−385.

BI0496687